Hindawi
International Journal of Digital Multimedia Broadcasting
Volume 2022, Article ID 2865659, 12 pages
https://doi.org/10.1155/2022/2865659

Research Article

Hybrid Beamforming Grouping Sum-Rate Maximization Algorithm for Multiuser mmWave Massive MIMO Systems

Jian Liu,[1] Xuan Yang,[1] Qianfang Sun,[1] Renmin Zhang,[1,2] and Yingjing Qian[1,2]

[1]*College of Information Science and Engineering, Jishou University, Jishou 416000, China*
[2]*Hunan Provincial Key Lab. of Intelligent Control Technology for Ecological Agriculture in Wuling Mountain Area, Huaihua University, Huaihua 418000, China*

Correspondence should be addressed to Renmin Zhang; rzhang1981@163.com and Yingjing Qian; qyingjing@163.com

Received 30 October 2021; Revised 19 December 2021; Accepted 10 January 2022; Published 10 February 2022

Academic Editor: Quoc-Tuan Vien

For multiuser millimeter wave (mmWave) massive multiple-input multiple-output (MIMO) systems, the key factor that causes the system sum-rate to change is its interference plus noise, corresponding to the number of base station (BS) antennas and signal-to-noise ratio (SNR) variation causing the system sum-rate changes, which in turn affects the user's communication quality. Based on this, this paper proposes an improved low-complexity hybrid beamforming grouping sum-rate maximization (HBG-SRM) algorithm to achieve system sum-rate maximization under the premise that both BS and user side use hybrid beamforming architecture and the channel state information (CSI) of the downlink channel is perfect. The algorithm first predefines a relevant threshold value, which is used to group multiusers; then, the user uses the maximum likelihood (ML) criterion to identify the optimal beam and estimate its beamforming gain within each group, and finally, the user compares all the candidate optimal beam gains between each group to confirm the optimal beamforming vector. The simulation results also verify the superiority of the proposed algorithm's sum-rate over other algorithms.

1. Introduction

As we all know, wireless signals are carried to radio waves for transmission in the air. From 2nd Generation (2G) to 4th Generation (4G), mobile communications are deployed to the low to medium frequency band below 6 GHz, which has a long wavelength, resulting in a wide coverage area, i.e., the golden frequency band for mobile communications. However, due to the large number of data services gathered in this band, the available spectrum resources are very limited. And with the advent of the 5th Generation (5G) mobile communications era, which needs to handle data transmission rates of the order of Gbps, it is obviously insufficient, and the opening of the millimeter wave (mmWave) band is indispensable [1–4]. mmWave communication has been widely concerned by academia and industry because of its abundant spectrum resources, and it has become one of the enabling technologies for Behind 5th Generation (B5G) and 6th Generation (6G) wireless communication systems [5–8]. Because of its ultra-high-frequency characteristics, the propagation distance of mmWave will naturally be shorter than that of the middle- and low-end frequency bands, and the signal transmission will also suffer serious path loss. Fortunately, the small wavelength of mmWave enables the deployment of massive antenna arrays at the transceiver side and the integration of terminals, so that the high path loss of mmWave signal transmission can be compensated by the beamforming gain generated by the massive multiple-input multiple-output (MIMO) technique [9–12].

The former 5G era was to enhance the signal transmission rate by increasing the signal transmitting power, but the power cannot be increased indefinitely, so beamforming technology came into being. Its advantages are obvious: (1) first of all, the signal can be propagated farther and more accurately; (2) greatly reduce the path loss, that is, saving the transmit power; and (3) reduce the interference between users of the same channel. However, there are many problems when put into the real environment. First, the real environment is different from free space, there will be a variety of obstacles, and mmWave because of its short wavelength is

more likely to be blocked than the low and medium frequency band, when a person walks behind the obstacles, triggering a non-line-of-sight (NLoS) long-range communication; the solution is to use beam tracking, beam steering, and beam switching technology. No matter how complex the environment is and how people move, the base station (BS) and the terminal can cooperate with each other to complete beam scanning pairing and finally select an optimal path to be used for communication [13–17]. Full-digital beamforming is characterized by the need to connect a dedicated Radio Frequency (RF) chain to each antenna; however, in mmWave massive MIMO systems, the number of antennas may reach several hundreds or more, which results in additional hardware complexity and power wastage [18–21]. This challenge can be solved by a hybrid beamforming architecture, which is the most promising approach to reduce the high hardware cost and power consumption by combining high-dimensional analog precoding with low-dimensional digital baseband precoding through a phase shifter, which is approximated as a problem of minimizing the Euclidean distance between a fully digital precoder and a hybrid precoder (the Euclidean distance is considered the degree of similarity of signals. The closer the distance, the more similar they are, the more likely they are to interfere with each other, and the higher the BER). This problem is further reduced to the matrix decomposition problem of the fully digital precoder, i.e., the product of the digital baseband precoder matrix and the analog RF precoder matrix [22–24].

Regarding some recent studies on localization and anti-interference for mmWave massive MIMO, a dynamic two-dimensional (2D) fingerprint training scheme based on maximum likelihood (ML) estimation and information entropy theory is proposed in [25] for robust localization problems in line-of-sight (LOS) and NLOS environments. A spatial information-based beam extraction method is proposed in [26] to eliminate the pilot contamination for the problem of resisting simultaneous eavesdropping and interference, and a beam-domain distributed reception scheme is proposed to suppress the interference in the user signal on this basis. The beam-domain antijamming transmission problem in downlink massive MIMO systems is studied in [27]. These studies are well able to combat interference for multiuser transmission. However, for the design of hybrid beamforming, the hybrid beamforming algorithm proposed in [28] is based on the idea of grouping, and in a multiuser mmWave MIMO system, an exhaustive algorithm is used to search within the divided group, and an avarice algorithm is then used between the groups to select the optimal beam, uplink channel is used, and the complexity of the exhaustive search is still very high. In [29], on the other hand, an avarice iterative approach is used, where an element of the analog beamforming matrix is majorizated only once. And in the multiuser systems, [30] gives another method for beam manipulation, where the beam set vector with the largest relevance to the channel vector is selected at the BS side for beamforming. However, this method cannot effectively suppress interuser interference. The forced-zero precoding algorithm proposed in [31] approximates the interuser interference as a Least-Square (LS) problem and uses the precoding matrix for interference cancellation. Since the effect of noise is not taken into account and the forced-zero effect is better only in the case of a high signal-to-noise ratio (SNR), it is obvious that the performance of this method is not optimal and cannot effectively eliminate interuser interference.

In this paper, we propose an improved low-complexity hybrid beamforming grouping sum-rate maximization (HBG-SRM) algorithm based on [28] to address the above problem. This algorithm can effectively reduce interuser interference and maximize the multiuser massive MIMO system sum-rate. Our main contributions to the paper are as follows:

(a) We propose an improved low-complexity hybrid beamforming grouping sum-rate maximization (HBG-SRM) algorithm, which is aimed at optimizing the sum-rate in multiuser scenarios. The algorithm is divided into three steps:

(i) The users are grouped according to the predefined relevant threshold value

(ii) The users use the ML criterion within each group to identify the optimal beam and estimate its beamforming gain

(iii) The users compare the gain of all candidate optimal beams among each group to confirm the optimal beamforming vector

(b) Based on the original plan, putting forward the improvement scheme can reduce the cost and complexity. This algorithm can effectively mitigate the interference between users and maximize the sum-rate in multiuser mmWave MIMO systems

(c) Based on the control variable method, the optimal values of system sum-rate of the HBG-SRM algorithm in practical application scenarios are verified from the relationship between system sum-rate and SNR of different algorithms in different fixed BS antenna number scenarios and the relationship between system sum-rate and BS antenna number of different algorithms in different fixed SNR scenarios

(d) We make a theoretical analysis of the factors that influence the sum-rate under the multiuser scenario, and it is concluded that the algorithm has a higher sum-rate under ideal channel conditions compared to other algorithms. At the same time, the suitable scenario and the future research direction of the algorithm are analyzed qualitatively for further development and research

The sections of the paper are organized as follows: Section 1 is an introduction to the research background and the current research status of the paper, with the aim of

introducing our proposed scheme for this problem. Section 2 specifies the adopted system model, covering the system architecture and the channel model. Section 3 elaborates the design problem of the scheme and the proposed HBG-SRM algorithm. The simulation results and algorithm complexity are analyzed in Section 4. Finally, the conclusion and future outlook of the paper are given in Section 5.

Notations. Bold uppercase and lowercase letters represent matrices and vectors, respectively, e.g., $\mathbf{A}$ and $\mathbf{a}$.Two-norm of $\mathbf{A}$ is denoted by $\|\mathbf{A}\|_2$; $|\mathbf{A}|$ denotes the modulus value of $\mathbf{A}$. The $N \times N$ identity matrix denotes as $\mathbf{I}_N$, $\mathscr{A}$ denotes the sets, and $|\mathscr{A}|$ denotes the cardinality of the sets $\mathscr{A}$, e.g., Card $(\cdot)$ represents the number of components. The transpose, Hermitian transpose, and inverse operators of $\mathbf{A}$ are denoted by $\mathbf{A}^T$, $\mathbf{A}^H$, and $\mathbf{A}^{-1}$, respectively. $\mathbb{C}$ denotes matrix sets.

2. System Model

In this section, we first give a detailed overview of the transmission characteristics of mmWave and the related knowledge of massive MIMO beamforming, in order to provide the necessary theoretical basis for the downlink communication between transmitter and receiver in the hybrid beamforming architecture later on. The channel model is elaborated in the last part of this section, all of which are intended to provide the necessary complementary explanations to the algorithms in Section 3 and the simulation results in Section 4 later.

2.1. mmWave Transmission Characteristics and Massive MIMO Beamforming

(1) The free-space path loss can be described by the Friesian free-space propagation loss equation [32]:

$$P_r = P_t \frac{G_t G_r \lambda^2}{(4\pi R)^2}, \tag{1}$$

where P_r, P_t denote the far-field received power and transmitted power, λ represents the antenna wavelength, d represents the antenna spacing, and G_r, G_t denote the directional transceiver antenna gain; it can be seen that under a fixed antenna aperture area, the transmission loss increases with the increase of frequency because the wavelength and frequency are inversely proportional to each other. And the loss of mmWave penetrating different media is shown in Table 1.

(2) 5G key technology-massive MIMO can be illustrated by the diagram shown in Figure 1, where equation (2) is Shannon's formula:

$$C = L \cdot B \log_2(1 + S/N), \tag{2}$$

where L denotes the number of channels, C denotes the system capacity, B denotes the channel bandwidth, and S/N is the signal-to-noise ratio (SNR).

Table 1: Loss of mmWave penetration through different media.

Materials	Thickness (cm)	Penetration loss (dB)
Wood	4.25~28	8.34~15.08
Drywall	6.5~37.25	11.85~53.47
Concrete	19~34.25	31.32~60.11

Digital beamforming refers to the use of beamforming techniques at the baseband, i.e., the use of precoding techniques at the baseband to form a phase difference between the signals emitted at each antenna, thus achieving beamforming effects. Therefore, digital beamforming is also called precoding. It has the following characteristics.

(1) Easy to implement when the number of antennas is small

(2) Easy to design complex algorithms

(3) Suitable for multilayer and multiuser

(4) High cost when the number of antennas is large

(5) High hardware requirements

Analog beamforming refers to the use of RF beamforming techniques at the RF, i.e., the use of phase shifters at the antennas to form a phase difference between the signals emitted at each antenna, thus achieving the effect of beamforming. Therefore, analog beamforming is also called RF beamforming, and it is easy to use when the number of antennas is large. It has the following characteristics.

(1) Reduced hardware complexity

(2) Reduced flexibility when the number of antennas is small

(3) Not easy to design complex algorithms

(4) MIMO scenarios cannot be implemented

Hybrid beamforming combines digital and analog techniques, allowing the advantages of both approaches to be exploited and the disadvantages to be compensated. Performance is balanced with cost and complexity. In short, the baseband part mainly implements MIMO and the RF part mainly implements beamforming [33–37].

2.2. System Architecture. As shown in Figure 2, a hybrid beamforming architecture is used at both the BS and User Equipment (UE) sides. The BS equipped with N_t antennas and N_t^{RF} RF chains communicates with K single-antenna users. Satisfying $N_s \le N_t^{\mathrm{RF}} < N_t$ and $N_s \le N_r^{\mathrm{RF}} < N_r$, assuming $N_t^{\mathrm{RF}} = K$, the aim is to make a good compromise between the performance and complexity of the system and to minimize the additional interference caused by hardware. The downlink channel is the ideal channel, i.e., the BS is fully aware of the channel state information (CSI). A schematic diagram is shown in Figure 3.

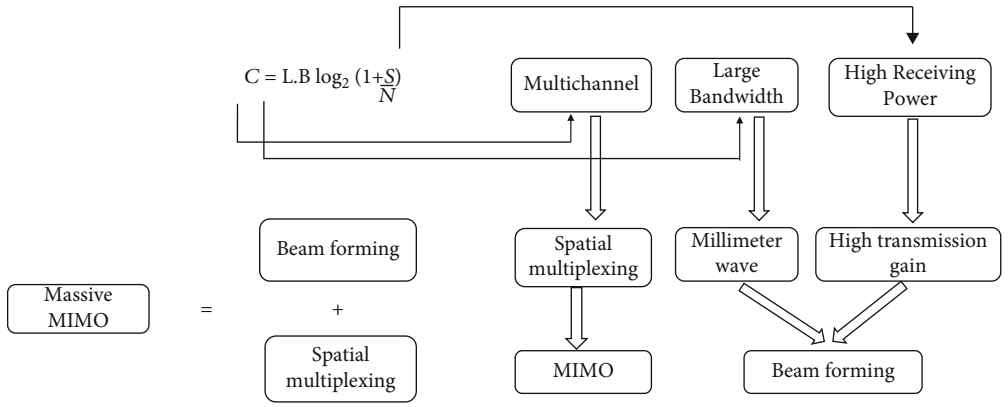

Figure 1: The key technology of 5G-massive MIMO.

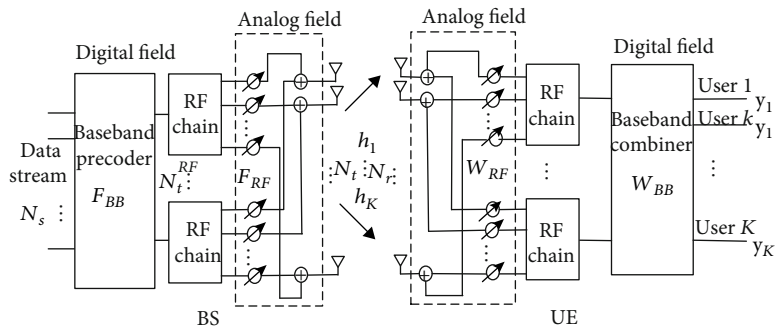

Figure 2: Millimeter wave multiuser MIMO hybrid beamforming system architecture.

At the transmitter side, the signal transmitted by the BS is first digitally precoded, which is processed in the baseband digital precoder $\mathbf{F}_{\mathrm{BB}}$ to generate the baseband signal, and then, the baseband signal is upconverted to the carrier frequency through the N_t^{RF} RF chain, and then, the phase of the antenna array element is controlled by the constant mode phase shifter in the analog beamformer $\mathbf{F}_{\mathrm{RF}}$ to realize the beamforming of the signal at the transmitter side. At the receiving end, after the signal arrives through the mmWave multipath sparse channel, it is firstly controlled by the constant mode phase shifter in the RF analog combiner $\mathbf{W}_{\mathrm{RF}}$ to control the phase of the antenna array element, so as to realize the beamforming of the signal at the receiving end, and the obtained signal is then demodulated by the baseband digital combiner $\mathbf{W}_{\mathrm{BB}}$. The final received signal needs to be processed by the receiver's combiner before it can be obtained completely. As in the hybrid beamforming system shown in Figure 2, the beamforming matrix $\mathbf{F} = \mathbf{F}_{\mathrm{RF}}\mathbf{F}_{\mathrm{BB}}$, where $\mathbf{F}_{\mathrm{BB}} \in \mathbb{C}^{\mathbf{N_s} \times \mathbf{N_t^{RF}}}$ denotes the baseband digital precoding matrix, $\mathbf{F}_{\mathrm{RF}} \in \mathbb{C}^{\mathbf{N_t} \times \mathbf{N_t^{RF}}}$ denotes the RF analog precoding matrix, and $\mathbb{C}$ denotes the set of matrices. The transmit signal of the antenna array element at the transmitter is $x = \mathbf{F}_{\mathrm{RF}}\mathbf{F}_{\mathrm{BB}}\mathbf{s}$, $\mathbf{s} \in \mathbb{C}^{\mathbf{N_s} \times \mathbf{1}}$ denotes the transmit signal vector and satisfies $\mathbf{E}[\mathbf{s}\mathbf{s}^H] = \boldsymbol{\rho}\mathbf{I}_{\mathbf{K}}/K$, $\mathbf{I}$ is the unit matrix, $E[\cdot]$ denotes the expectation, ρ denotes the signal transmit power, and for the power limit, $\|\mathbf{F}_{\mathrm{RF}}\mathbf{F}_{\mathrm{BB}}\|_F^2 = \boldsymbol{N_s}$ needs to be satisfied, where $\|\cdot\|_F^2$ denotes the matrix norm, and since $\mathbf{F}_{\mathrm{RF}}$ only changes

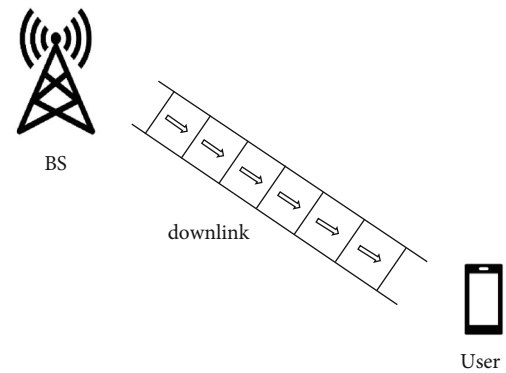

Figure 3: Schematic diagram of downlink communication.

the phase of the signal, it satisfies $|\mathbf{F}_{\mathrm{RF}}(i,j)| = 1/\sqrt{N_t}$. After processing through the RF analog combined matrix $\mathbf{W}_{\mathrm{RF}} \in \mathbb{C}^{\mathbf{N_r} \times \mathbf{N_r^{RF}}}$ and the baseband digital combined matrix $\mathbf{W}_{\mathrm{BB}} \in \mathbb{C}^{N_r^{\mathrm{RF}} \times \mathbf{N_s}}$ at the receiver, the kth user's received signal can be represented as

$$\begin{aligned}\mathbf{y}_k = {} & \sqrt{\mathbf{p}}\mathbf{W}_{\mathrm{BB}}^{(k)H}\mathbf{W}_{\mathrm{RF}}^{(k)H}\mathbf{H}_k\mathbf{F}_{\mathrm{RF}}^{(k)}\mathbf{F}_{\mathrm{BB}}^{(k)}\mathbf{s}_k \\ & + \sum_{i=1, i\neq k}^{K} \sqrt{\mathbf{p}}\mathbf{W}_{\mathrm{BB}}^{(k)H}\mathbf{W}_{\mathrm{RF}}^{(k)H}\mathbf{H}_k\mathbf{F}_{\mathrm{RF}}^{(i)}\mathbf{F}_{\mathrm{BB}}^{(i)}\mathbf{s}_i \\ & + \mathbf{W}_{\mathrm{BB}}^{(k)H}\mathbf{W}_{\mathrm{RF}}^{(k)H}\mathbf{n}_k,\end{aligned} \tag{3}$$

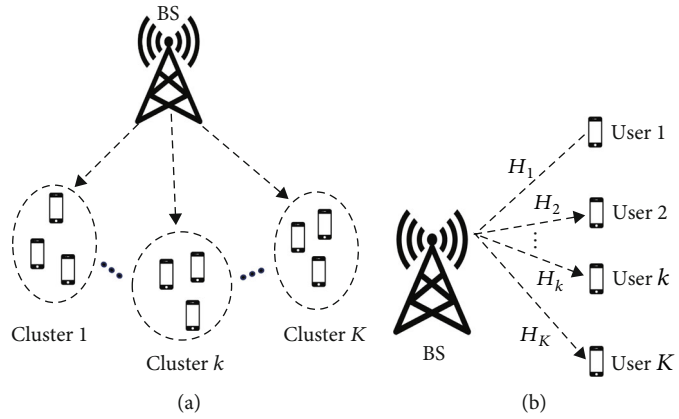

Figure 4: (a) Schematic diagram of narrowband clustering multipath sparse channel model from BS to user. (b) Diagram of a multiuser channel from BS to user.

where the first term on the right side of the equation is the signal expected to be received by the user, the second term is the interference term of other users, and the last term is the noise term. $\mathbf{H}_k = [\mathbf{h}_1, \mathbf{h}_2, \cdots, \mathbf{h}_K] \in \mathbb{C}^{N_r \times K}$ represents the kth channel matrix from the BS to the user, and $\mathbf{h}_K \in \mathbb{C}^{N_r \times \mathbf{1}}$ is the channel vector of the kth user. $\mathbf{n} \in \mathbb{C}^{N_r \times 1}$ represents the complex Gaussian white noise vector, obeying $\mathscr{C}\mathcal{N}(\mathbf{0}, \sigma^2 \mathbf{I}_{N_r})$, $\mathbf{F}_{\mathrm{BB}}$, $\mathbf{W}_{\mathrm{BB}}$ can be designed by the Minimum Mean Square Error (MMSE) criterion in [28, 30], i.e.,

$$\mathbf{F}_{\mathrm{BB}} = \mathbf{H}\wedge^{*}\left(\mathbf{H}\wedge\mathbf{H}\wedge^{*}\right)^{-1}, \tag{4}$$

$$\mathbf{W}_{\mathrm{BB}} = \widehat{\mathbf{H}}\left(\mathbf{H}\wedge^{\mathbf{H}}\mathbf{H}\wedge + \mathbf{I}_K\right)^{-1}, \tag{5}$$

where $\widehat{\mathbf{H}} = \mathbf{F}_{\mathrm{RF}}^{H}\mathbf{H} \in \mathbb{C}^{K\times K}$. And we indicate the sum-rate as follows [38]:

$$R = \sum_{k=1}^{K} \log_2(1 + \mathrm{SINR}_k), \tag{6}$$

$$\mathrm{SINR}_k = \frac{P/K\left|\mathbf{h}_k^H \mathbf{F}\mathbf{w}_k\right|^2}{1 + \sum_{j\neq k} P/K\left|\mathbf{h}_k^H \mathbf{F}\mathbf{w}_j\right|^2}, \tag{7}$$

where SINR_k represents the kth user's Signal-to-Interference-Plus-Noise Ratio (SINR) and $\mathbf{w}_j$ denotes the jth column of $\mathbf{W}$.

2.3. Channel Model. The SV (Saleh-Valenzuela) geometric channel model is used [39, 40]. It is a narrowband split-cluster multipath sparse channel model, as shown in the schematic diagram in Figures 4(a) and 4(b). Each user has N_{cl} scattering clusters, and each scattering cluster has N_p propagation paths. Each user corresponds to one channel.

Then, the kth user's channel matrix is indicated as

$$\mathbf{H}_k = \sqrt{\frac{N_r N_t}{N_{\mathrm{cl}} N_p}} \sum_{i,l} \alpha_{il} \mathbf{a}_R\left(N_r, \phi_{\mathbf{il}}^{\mathbf{k}}\right) \mathbf{a}_T{}^{H}\left(N_t, \theta_{\mathbf{il}}^{\mathbf{k}}\right), \tag{8}$$

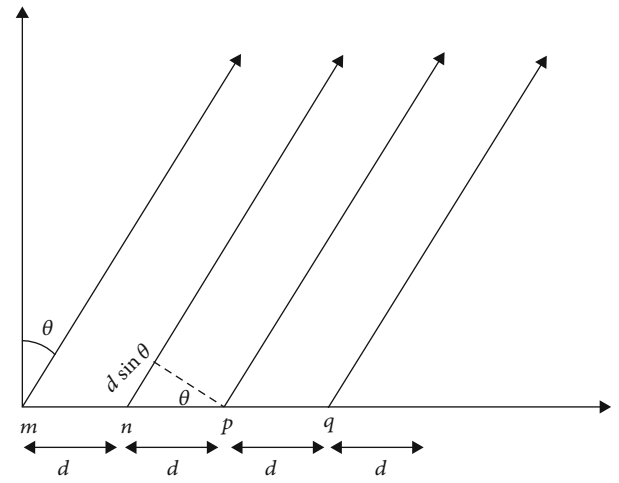

Figure 5: Massive MIMO-beam steering schematic diagram.

where α_{il} denotes the complex gain of the lth path within the ith cluster, $\mathbf{a}_T(N_t, \theta_{\mathbf{il}}^{\mathbf{k}})$, $\mathbf{a}_R(N_r, \phi_{\mathbf{il}}^{\mathbf{k}})$ are defined as the Array Response Vector (ARV) at the BS and the user end, and θ_{il} and ϕ_{il} are the Departure of Angles (DoA) and Arrival of Angles (AoA).

As shown in Figure 5 of the massive MIMO beam steering schematic, the distance between the antenna vibrators is d, the direction of the main flap of the transmitted signal and the vertical direction of the vibrator link (positive front) into θ angle then: the time difference between a vibrator n and its neighboring vibrator p transmitted signal

$$\tau = \frac{d \sin\theta}{c}. \tag{9}$$

The phase difference $\Delta\varphi = \omega\tau$ between vibrator n and vibrator p, i.e., $\varphi = \omega((d \sin\theta)/c)$, and since $\omega = 2\pi f$, $f = c/\lambda$, substitution gives $\Delta\varphi = 2\pi(c/\lambda)\ ((d \sin\theta)/c) = ((2\pi)/\lambda)d \sin\theta$, and when $d = \lambda/2$, we have $\Delta\varphi = \pi \sin\theta$, and the BS uses a Uniform Linear Array (ULA) to receive the signal; the ARV is expressed as

Proposed ADS-MBT scheme.
1.**Input**: N_t, K, N_{cl}, N_p;
2.**Output**: The optimal beamforming vector $\{\mathbf{f}^{**}, \mathbf{w}^{**}\}$;
3.**Set**: Correlation $[\mathbf{C}]_{\mathbf{i,l}}$ by (13), extract index i, l by (14);
4.**Calculation**: correlation threshold e_{u_i} by (15);
5.**Options**: $S_{u_i} = \{l \mid [\mathbf{C}]_{u_i,l} > e_{u_i}, l \in \Delta\}$, from the remaining $K - i$ users , form a set S_{u_i}; let $\Theta_i = S_{u_1} \cap S_{u_2} \cap \cdots S_{u_i}$; represents the candidate set of the $i+1$ element in G;
6.**Determine:** If $\mathrm{Card}(\Theta_i) = 0$, G has only i elements. If $\mathrm{Card}(\Theta_i) = 1$, the $(i+1)$th element in G is a member of Θ_i. If $\mathrm{Card}(\Theta_i) > 1$, $\Theta_i = (k_1, k_2, \cdots, k_j)$, determine the $(i+1)$th element u_{i+1} in G according to (17) and (18);
7.**Update**: $e_{u_{i+1}}$ 、 $S_{u_{i+1}}$, Θ_{i+1} by (15), (16), repeat the process until the group is complete;
8.**Grouping:** Repeat (14)–(18) to group the remaining users until all users are grouped;
9.**Intragrouping Identification:** From (19) to (22), ML criterion is used in each group to identify the optimal beam and estimate its beamforming gain;
10. **Intergrouping Confirmation**: The gain of all candidate optimal beams is compared between each group by (23) to confirm the optimal beamforming vector $\{\mathbf{f}^{**}, \mathbf{w}^{**}\}$, BS uses it for downlink transmission.

Algorithm 1: HBG-SRM algorithm.

$$\mathbf{a}_T\left(N_t, \theta_{\mathbf{il}}^{\mathbf{k}}\right) = \frac{1}{\sqrt{N_t}}\left[1, \mathbf{e}^{\mathbf{j}(2\Pi/\lambda)d \sin\left(\theta_{\mathbf{il}}^{\mathbf{k}}\right)}, \cdots, \mathbf{e}^{\mathbf{j}(N_t-1)(2\Pi/\lambda)d \sin\left(\theta_{\mathbf{il}}^{\mathbf{k}}\right)}\right]^T,$$

$$\mathbf{a}_R\left(N_r, \phi_{\mathbf{il}}^{\mathbf{k}}\right) = \frac{1}{\sqrt{N_r}}\left[1, \mathbf{e}^{\mathbf{j}(2\Pi/\lambda)d \sin\left(\phi_{\mathbf{il}}^{\mathbf{k}}\right)}, \cdots, \mathbf{e}^{\mathbf{j}(N_r-1)(2\Pi/\lambda)d \sin\left(\phi_{\mathbf{il}}^{\mathbf{k}}\right)}\right]^T. \tag{10}$$

From this, we can also draw the following conclusions.

(1) Multiple antenna vibrators in parallel can make the transmitted signal form directional-beamforming

(2) The relative phase change between multiple vibrators makes the direction of the transmitted signal change-beam steering

3. Proposed HBG-SRM Algorithm

In this section, the proposed HBG-SRM algorithm is described systematically, starting with a specific description of the problem, followed by a detailed exposition of the specific details of the algorithm, and at the end of this section, the algorithm is summarized in Algorithm 1.

3.1. Problem Description. From equations (4) and (5), we know that $\mathbf{F}_{\mathrm{BB}}$ and $\mathbf{W}_{\mathrm{BB}}$ can be obtained from $\mathbf{F}_{\mathrm{RF}}$ and $\mathbf{H}$ [28]. That is, the design of the hybrid beamforming matrix is converted into the design of $\mathbf{F}_{\mathrm{RF}}$, i.e.,

$$\mathbf{F}_{\mathrm{RF}} = \arg\max_{\mathbf{F}_{\mathrm{RF}}} \sum_{k=1}^{K} \log_2(1 + \mathrm{SINR}_k), \quad \text{s.t.}\mathbf{f} \in \mathscr{F}, \mathbf{w} \in \mathscr{W}, \tag{11}$$

where $\mathscr{F}$, $\mathscr{W}$ are predefined codebook sets and $\mathbf{f}$, $\mathbf{w}$ are feasible beamforming vectors, denoted as

Table 2: Simulation parameters.

Simulation parameters	Value
Number of BS antennas N_t	$[8 : 16 : 32 : 64]$
Number of user antennas N_r	8
Antenna distance d	0.5λ
Number of users K	8
N_{cl}	8
N_p	10
SNR	$[-20 : 5 : 20]$

$$\mathscr{F} = \left\{\mathbf{a}\left(N_t, \theta_k^t\right) \mid \cos\theta_k^t = \frac{2k - 1 - N_t}{N_t}, k = 1, 2, \cdots, N_t\right\},$$
$$\mathscr{W} = \left\{\mathbf{a}\left(N_r, \theta_k^r\right) \mid \cos\theta_k^r = \frac{2k - 1 - N_r}{N_r}, k = 1, 2, \cdots, N_r\right\}. \tag{12}$$

The above equation can be directly used to obtain the optimal solution by the exhaustive method. However, in a multiuser MIMO scenario, the large number of antennas at the BS side implies a high degree of complexity. Therefore, we propose an improved low-complexity HBG-SRM algorithm.

3.2. Multiuser Grouping. From equation (3), it is known that in a multiuser mmWave massive MIMO system, the kth user will suffer interference from $(k-1)$th users. Based on [28], the correlation between the user channel vectors is used to measure the interference strength. The correlation is represented by the matrix $\mathbf{C} \in \mathbb{R}^{K \times K}$, i.e.,

$$[\mathbf{C}]_{i,l} = \begin{cases} \left|h_i^{\mathrm{H}} h_l\right|^2, & i \neq l, \\ 0, & i = l, \end{cases} \tag{13}$$

where $[\mathbf{C}]_{i,l}$ denotes the relevance between the ith user and the lth user, from which we extract the ordinal value corresponding to the largest element as users u_1 and u_2, i.e.,

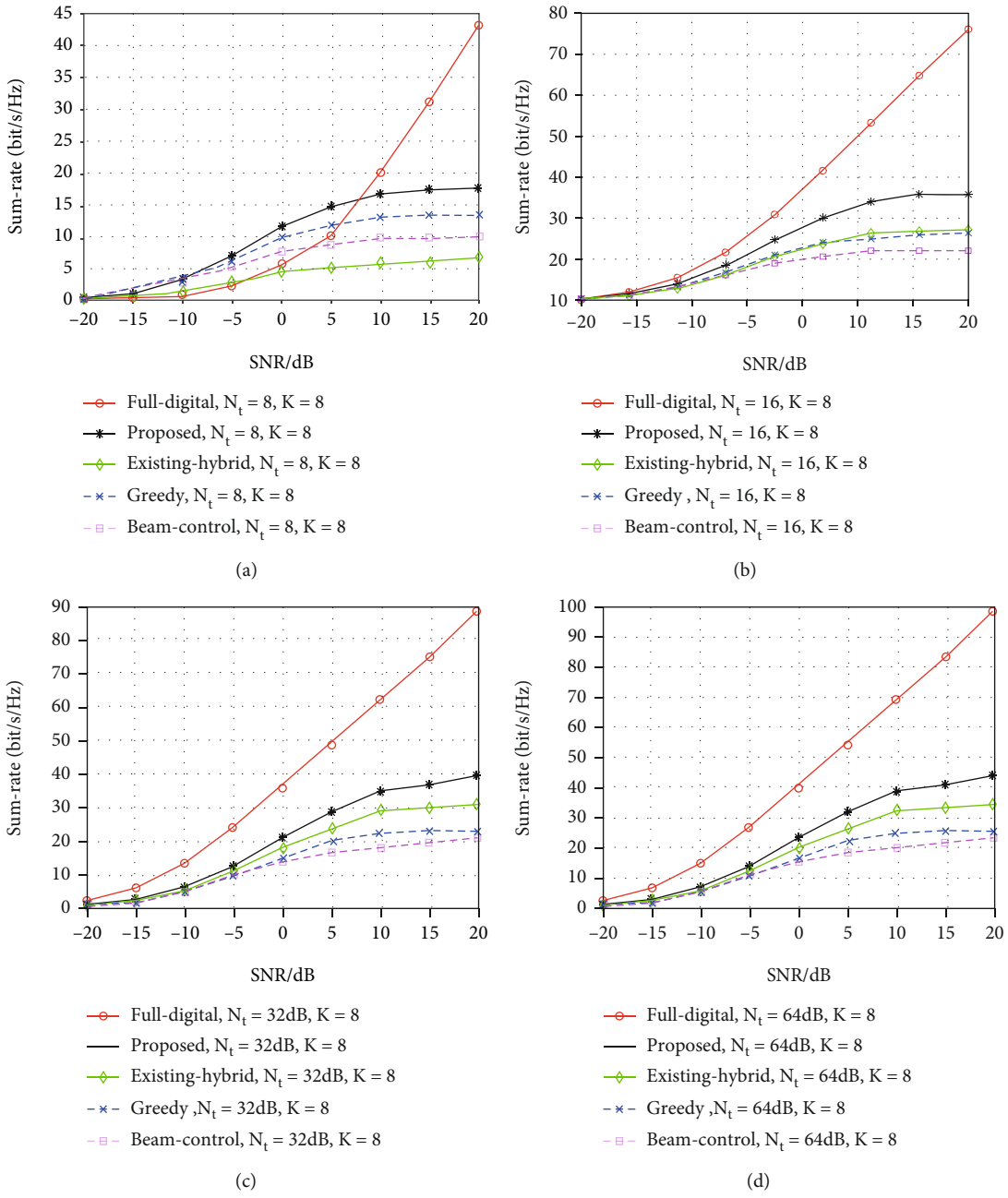

Figure 6: The system sum-rate versus SNR ratio diagram of different algorithms in different fixed BS antenna scenarios.

$$(u_1, u_2) = \arg \max_{i,l} [\mathbf{C}]_{i,l}. \tag{14}$$

Put users u_1 and u_2 in a group, represented by set G, that is, $G = (u_1, u_2)$. Then consider whether to add user u_i to G, $i > 2, i \in \mathbb{Z}$. User u_i relevance threshold e_{u_i} is defined as the average value between user u_i and other users, given by

$$e_{u_i} = \sum_{j=1}^{K} \frac{[\mathbf{C}]_{u_i,j}}{K}. \tag{15}$$

Next, we select the users whose relevance with u_i is greater than the threshold value from the $(K - i)$ users whose index value has never been extracted and represent them by set S_{u_i}, where l and Δ represent the serial number and sequence set of the remaining users, respectively:

$$S_{u_i} = \left\{ l \mid [\mathbf{C}]_{u_i,l} > e_{u_i}, l \in \Delta \right\}. \tag{16}$$

Let $\Theta_i = S_{u_1} \cap S_{u_2} \cap \cdots S_{u_i}$. Take it as the set of $(i+1)$th candidate index values in set G. The next step is to judge whether to put the $(i+1)$th candidate index value into set

G. If $\mathrm{Card}(\Theta_i) = 0$, G has only i index values. If $\mathrm{Card}(\Theta_i) = 1$, the $(i+1)$th candidate index values in set G is a member of Θ_i. If $\mathrm{Card}(\Theta_i) > 1$, $\Theta_i = (k_1, k_2, \cdots k_j)$, judge the $(i+1)$th candidate index value u_{i+1} in set G by

$$Q_k = [\mathbf{C}]_{u_1,k} + [\mathbf{C}]_{u_2,k} + \cdots + [\mathbf{C}]_{u_i,k}, k \in \Theta_i, \tag{17}$$

$$u_{i+1} = \arg \max_k Q_k. \tag{18}$$

Repeat (14)–(18), update $e_{u_{i+1}}$, $S_{u_{i+1}}$, and update $\Theta_{i+1} = \Theta_i \cap S_{u_{i+1}}$, to take it as the set of $(i+2)$th candidate index values in set G. The most relevant users were grouped. The last thing you need to do is loop through the process until the kth user is grouped.

3.3. Intragroup Identification and Intergroup Confirmation. By grouping above, if the exhaustive algorithm is used to select the optimal beam within each group, it will undoubtedly increase the algorithm's extremely high complexity. Nevertheless, in mmWave sparse multipath channels, the path gain of many paths are small and usually negligible. Therefore, only the beamforming vector corresponding to the large path gain needs to be selected. That is, the user uses the maximum likelihood (ML) criterion within each group to identify the optimal beam and estimate its beamforming gain:

$$\left\{\mathbf{f}_g^\star, \widehat{q}_{g,f_g^\star}\right\} = \arg \min_{1 \le f_g \le N_g} \left\| \mathbf{y}_g - q\left(\mathbf{w}_g\left(\mathbf{f}_g, :\right)\right)^H \right\|_2, \tag{19}$$

$$\widehat{q}_{g,f} = N_g \mathbf{y}_g^H \left(\mathbf{w}_g\left(\mathbf{f}_g, :\right)\right)^H, \tag{20}$$

where $\mathbf{y}_g, q_{g,f}, \mathbf{f}_g^\star$ denote the received signal vector, beamforming gain, and candidate optimal beamforming vector of the gth group, respectively, $\star$ denotes the best, and N_g denotes the number of beamforming vectors of the gth group. Using the ML criterion, the above equation is equivalent to

$$\mathbf{f}_g^\star = \arg \max_{1 \le f_g \le N_g} \left| \widehat{q}_{g,f} \right|, \tag{21}$$

$$\widehat{q}_{g,f_g^\star} = N_g \mathbf{y}_g^H \left(\mathbf{w}_g\left(\mathbf{f}_g^\star, :\right)\right)^H. \tag{22}$$

Finally, the user compares the gain of all candidate optimal beams between each group to confirm the optimal beamforming vector:

$$\mathbf{f}_g^{\star\star} = \arg \max_{1 \le g \le G} \left| \widehat{q}_{g,f_g^\star} \right|, \tag{23}$$

where $\mathbf{f}_g^{\star\star}$ denotes the optimal beamforming vector. The above process is repeated until the optimal beamforming vector is selected. From equation (6), the system sum-rate R_g for the gth group are obtained. The optimal beamforming vector is expressed as

Table 3: Simulation parameters.

Simulation parameters	Value
Number of BS antennas N_t	[20 : 5 : 65]
Number of user antennas N_r	8
Antenna distance d	0.5λ
Number of users K	8
N_{cl}	8
N_p	10
SNR	[5 : 10 : 15 : 20]

$$\left\{\mathbf{f}^{**}, \mathbf{w}^{**}\right\} = \arg \max_{\mathbf{f} \in \mathscr{F}, \mathbf{w} \in \mathscr{W}} R_g. \tag{24}$$

$\left\{\mathbf{f}^{**}, \mathbf{w}^{**}\right\}$ is used for downlink transmission. The proposed algorithm is summarized in Algorithm 1.

4. Simulation Results and Algorithm Complexity Analysis

In this section, we analyze the performance of the proposed algorithm, mainly by simulating its algorithm in terms of both SNR and number of antennas at the BS using the control variable method, and the simulation results confirm the superiority of the proposed algorithm. Then, we performed a complexity analysis of the algorithm, which also shows that the complexity of the system is within the tolerable range with increased system sum-rate. At the end of this section, we also provide an outlook on the shortcomings of the proposed algorithm for further development work.

4.1. Analysis of Simulation Results. Our proposed HBG-SRM scheme can be applied to mmWave communications where the known multipath components are very limited. To capture this weak scattering characteristic, we use the SV geometric channel model in the simulation. Based on the control variable method, we analyze the impact of different SNRs on the system sum-rate from different fixed BS antenna numbers, respectively. The system sum-rate of the full-digital algorithm, the existing hybrid beamforming algorithm, the greedy algorithm in [29], and the beam control algorithm in [30] are also compared. The specific simulation scenario parameters are in Table 2.

Figure 6 shows the system sum-rate versus SNR for different algorithms for different fixed BS antenna number scenarios. As shown in the figure, the sum-rate of all algorithms increases with the increase of SNR. The system sum-rate of the all-digital algorithm is the highest, which comes at the cost of high hardware complexity and large hardware overhead, which is not desirable in practice. It can be seen that the overall sum-rate of the system is not high when the number of antennas at the BS is small, and as the number of antennas increases to a certain value, such as to 64, the curve of the algorithm flattens out and the sum-rate of the system reaches the highest. In other words, at high SNR, for the performance of the proposed algorithm, although there is a

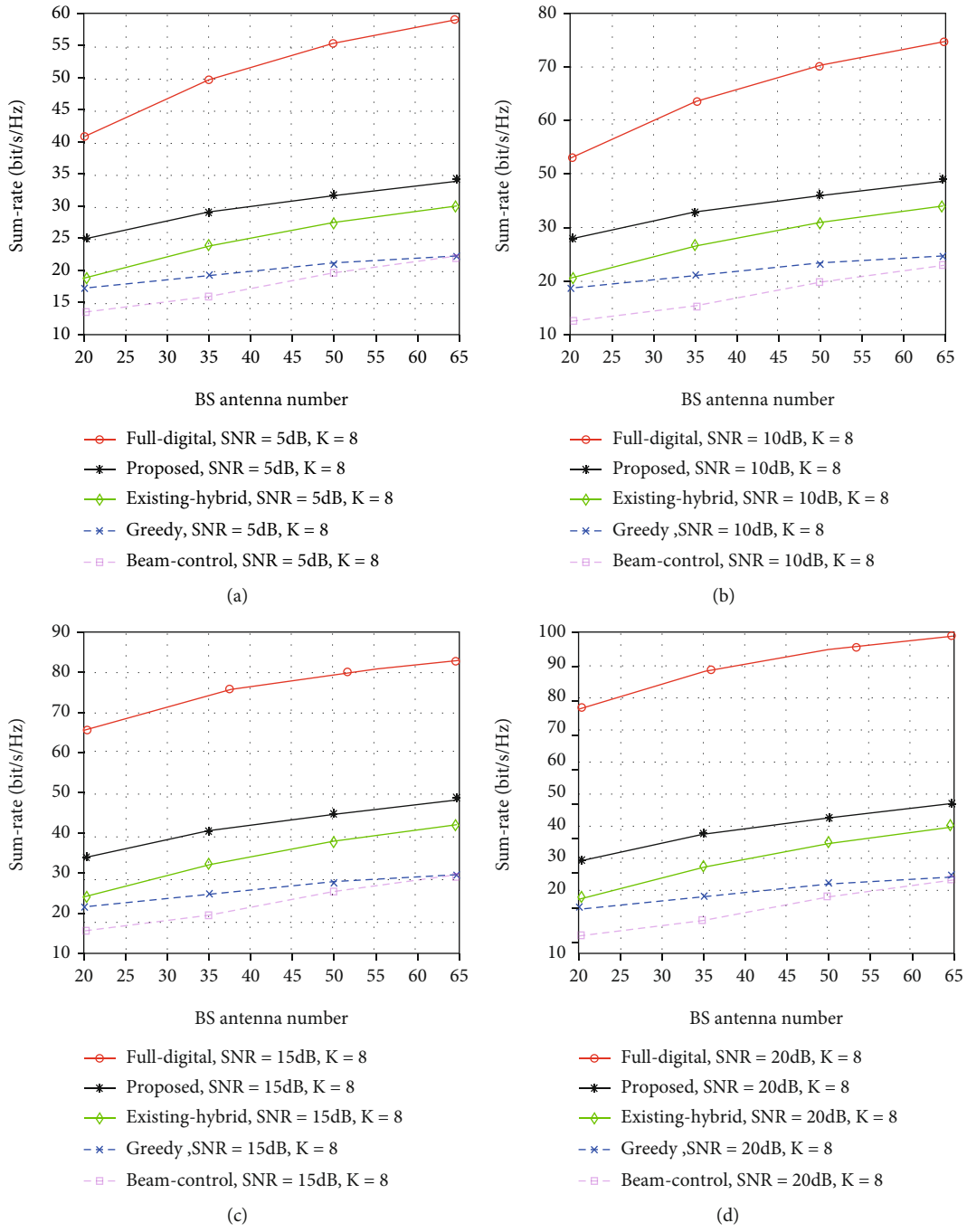

Figure 7: The system sum-rate versus BS antenna number ratio diagram of different algorithms in different fixed SNR scenarios.

certain difference compared with the performance of the all-digital algorithm, the complexity is greatly reduced and the performance is better than the existing hybrid beamforming algorithm and the beam control algorithm proposed in [30] and the greedy algorithm proposed in [29]. In particular, the system sum-rate of the HBG-SRM algorithm reaches close to 50 bit/s/Hz when $N_t = 64$ and SNR = 20 dB.

We also simulate the effect of different numbers of BS antennas on the system sum-rate from different fixed SNR scenarios, respectively. And it is also analyzed and compared with the sum-rate of the all-digital algorithm, the existing hybrid beamforming algorithm, the greedy algorithm in [29], and the beam control algorithm in [30]. The specific simulation scenario parameters are in Table 3.

Figure 7 shows the simulation plots of the system sum-rate versus the number of BS antennas for different algorithms for different fixed SNR scenarios. As shown in the figure, the HBG-SRM algorithm achieves a good compromise between performance and complexity, and the sum-rate of all algorithms increases with the number of BS antennas. As can be seen from the figure, with the increase of SNR (here, we do not consider the case of very low SNR because

Table 4: Algorithm complexity analysis.

Algorithm	Multiplication formula
Full-digital	$n \times \left(K\left(N_r^{\mathrm{RF}} N_r N_t N_t^{\mathrm{RF}} N_s\right) + (K-1)\left(N_r^{\mathrm{RF}} N_r N_t N_t^{\mathrm{RF}} N_s\right) + \cdots + N_r^{\mathrm{RF}} N_r N_t N_t^{\mathrm{RF}} N_s\right)$
Greedy	$n \times \left(K N_r^{\mathrm{RF}} N_r N_t N_s + N_t^2 N_r^{\mathrm{RF}} N_s + N_t N_t^{\mathrm{RF}}\left(N_r^{\mathrm{RF}} + N_t\right) N_s\right) + K\left(N_r N_t N_t^{\mathrm{RF}} N_s + N_r N_t^{\mathrm{RF}}\left(N_r + N_t^{\mathrm{RF}}\right) N_s + N_r^2 N_t^{\mathrm{RF}} N_s\right)$
Beam control	$n \times \left(K\left(N_r^{\mathrm{RF}} N_r N_t N_t^{\mathrm{RF}}\right) N_s + K\left(N_r - N_t^{\mathrm{RF}} + 1\right) N_s + K\left(N_t - N_r^{\mathrm{RF}} + 1\right) N_s\right)$
Existing hybrid	$n \times \left(K N_r (N_r - 1) N_s \cdots \left(N_r - N_t^{\mathrm{RF}} + 1\right) N_s + K N_r N_t^{\mathrm{RF}} N_t N_s\right)$
Proposed	$n \times \left(K\left(N_r^{\mathrm{RF}} N_r + N_t^{\mathrm{RF}} N_t\right) N_s + K^2 N_r^{\mathrm{RF}} N_r N_t N_t^{\mathrm{RF}} N_s + K\left(N_r^{\mathrm{RF}} N_t + N_t^{\mathrm{RF}} N_r\right) N_s\right)$

the system sum-rate is very low at this time), the system sum-rate of different algorithms improves rapidly with the increase of the number of BS antennas, and at SNR = 20 dB, the curve of this algorithm flattens out and the system sum-rate reaches the highest. In other words, the HBG-SRM algorithm is not as good as the performance of the all-digital algorithm, but it has better performance than the existing hybrid beamforming algorithm. When $N_t = 64$ and SNR = 20 dB, the difference between the system sum-rate of the proposed algorithm and the greedy algorithm in [29] is 20 bit/s/Hz. The system sum-rate of the HBG-SRM algorithm reaches close to 50 bit/s/Hz.

In summary, based on the control variable method, it can be seen from the system sum-rate versus SNR curves of different algorithms in different fixed BS antenna number scenarios and the system sum-rate versus BS antenna number in different fixed SNR scenarios that the system sum-rate of the HBG-SRM algorithm reaches the best when the number of BS antennas is 64 and the SNR is 20 dB, i.e., the optimal value of the algorithm in the practical application scenario is approximated as $N_t = 64$ and SNR = 20 dB.

4.2. Complexity Analysis. In Section 3, we give the specific steps of the algorithm, and in order to analyze the performance of the algorithm proposed in this paper, we give the complexity of several algorithms and the shortcomings of the algorithm in a multiuser mmWave massive MIMO communication system scenario. First of all, the computational complexity of several algorithms is analyzed. The innovation of the proposed algorithm is its improvement based on the grouping based on [28], which uses the exhaustive and greedy algorithms to select the optimal beam, because exhaustive and greedy searches are more time-consuming, so here, the computational complexity is mainly measured by the number of joint additions and multiplications performed during the ML criterion, assuming that n denotes the total number of cycles performed by the algorithm. The computational complexity of the algorithm is shown in Table 4. It can be seen that the complexity of the algorithm in this paper is slightly higher than that of the existing hybrid beamforming algorithm but much lower than that of the full complexity, greedy algorithm, and beam control algorithm. This also means that the HBG-SRM algorithm can provide higher performance with a small number of RF links equipped, i.e., within an acceptable complexity range, and is more cost-effective than the existing algorithms, achieving a compromise between complexity and performance.

However, the proposed algorithm has high requirements for the integrity of the channel state information, the realistic mmWave channel has time-varying characteristics, and the complex and variable receiver-side conditions (user's movement, location, speed, etc.) can also have an impact on the received signal, so it is difficult to obtain a better sum-rate under ideal conditions, and the algorithm is not suitable for single-UE beam refinement but more suitable for multi-UE initial access. Therefore, a future research direction could consider the use of wireless backhaul combined with cooperative relaying techniques for mmWave communication. This also implies that further analysis and research on hybrid precoding optimization problems are needed.

5. Conclusion and Outlook

In this paper, we propose an improved low-complexity hybrid beamforming grouping sum-rate maximization algorithm, which is aimed at optimizing the sum-rate in multiuser scenarios and reducing interference between users. The algorithm first predefines a relevant threshold value, which is used to group multiusers, then uses the ML criterion to identify the optimal beam and estimate its beamforming gain within each group. Finally, the user compares all candidate optimal beam gains within the divided group to confirm this optimal beam. The simulation consequences also verify the superiority of the proposed algorithm's sum-rate over other algorithms.

It is foreseeable that the future of 8 K resolution, Virtual Reality (VR), autonomous driving, live concert connectivity, smart manufacturing, and other typical 5G application scenarios must rely on the large bandwidth, low latency, and high capacity characteristics of mmWave to better achieve. However, a few years ago, mmWave communication on mobile devices was once considered by many to be absolutely impossible to achieve, but today, there are already many first-tier manufacturers on the market, launching commercial smartphones supporting mmWave; as can be seen from the relevant data this year, the global average downlink transmission rate of cell phones this year is only about 35 Mbps, while in areas where mmWave has been deployed, the average downlink rate of cell phones equipped with Snapdragon 5G mmWave solution is 900 Mbps, and the peak rate is 2 Gbps; besides cell phones, Snapdragon 5G mmWave solution is supporting a large number of Customer Premise Equipment (CPE), 5G modules, and even

PCs to enter our lives, and it is predictable that mmWave are not far from our life after successfully overcoming several well-known problems such as coverage range and NLoS communication [41–45].

Data Availability

The data used to support the findings of this study are available from the corresponding authors upon request.

Conflicts of Interest

The authors declare that they have no conflicts of interest.

Acknowledgments

This work is supported by the National Natural Science Foundation of China under grant 62061017, NSF of Hunan Province under grant 2021JJ30556, Educational Commission of Hunan Province under grant 19B456, and Postgraduate Scientific Research Innovation Project of Hunan Province under grants CX20201063 and QL20210244.

References

[1] R. W. Heath, N. Gonzalez-Prelcic, S. Rangan, W. Roh, and A. M. Sayeed, "An overview of signal processing techniques for millimeter wave MIMO systems," *IEEE Journal of Selected Topics in Signal Processing*, vol. 10, no. 3, pp. 436–453, 2016.

[2] B. R. Devi, B. Kiranmai, K. Gurucharan, S. S. Kiran, and P. Srujana, "A Coherent Hybrid Precoding for homogenize Millimeter-wave Multiple- in Multiple- out Systems for 5G Communication," in *2021 5th International Conference on Computing Methodologies and Communication (ICCMC)*, pp. 207–211, Erode, India, 2021.

[3] H. Xie, F. Gao, and S. Jin, "An overview of low-rank channel estimation for massive MIMO systems," *IEEE Access*, vol. 4, pp. 7313–7321, 2016.

[4] W. Chen, X. Ma, Z. Li, and N. Kuang, "Sum-rate maximization for intelligent reflecting surface based terahertz communication systems," in *2019 IEEE/CIC International Conference on Communications Workshops in China (ICCC Workshops)*, pp. 153–157, Changchun, China, 2019.

[5] W. Roh, J. Y. Seol, J. Park et al., "Millimeter-wave beamforming as an enabling technology for 5G cellular communications: theoretical feasibility and prototype results," *IEEE Communications Magazine*, vol. 52, no. 2, pp. 106–113, 2014.

[6] S. H. Faisal, S. Saleem, S. Shahid, and S. Saeed, "5G linear array for millimeter wave mobile communication in ultra dense networks (UDNs)," in *2019 International Conference on Electrical, Communication, and Computer Engineering (ICECCE)*, Swat, Pakistan, 2019.

[7] C. Feng, W. Shen, X. Gao, J. An, and L. Hanzo, "Dynamic hybrid precoding relying on twin- resolution phase shifters in millimeter- wave communication systems," *IEEE Transactions on Wireless Communications*, vol. 20, no. 2, pp. 812–826, 2021.

[8] A. Koc and T. Le-Ngoc, "Swarm intelligence based power allocation in hybrid millimeter-wave massive MIMO systems," in *2021 IEEE Wireless Communications and Networking Conference (WCNC)*, Nanjing, China, 2021.

[9] T. Bai and R. W. Heath, "Coverage and rate analysis for millimeter-wave cellular networks," *IEEE Transactions on Wireless Communications*, vol. 14, no. 2, pp. 1100–1114, 2015.

[10] F. Sohrabi and W. Yu, "Hybrid analog and digital beamforming for mmWave OFDM large-scale antenna arrays," *IEEE Journal on Selected Areas in Communications*, vol. 35, no. 7, pp. 1432–1443, 2017.

[11] S. Zhang, C. Guo, T. Wang, and W. Zhang, "On–Off analog beamforming for massive MIMO," *IEEE Transactions on Vehicular Technology*, vol. 67, no. 5, pp. 4113–4123, 2018.

[12] J. Qiao, X. Shen, J. W. Mark, and Y. He, "MAC-layer concurrent beamforming protocol for indoor millimeter-wave networks," *IEEE Transactions on Vehicular Technology*, vol. 64, no. 1, pp. 327–338, 2015.

[13] S. Noh, M. D. Zoltowski, and D. J. Love, "Multi-resolution codebook and adaptive beamforming sequence design for millimeter wave beam alignment," *IEEE Transactions on Wireless Communications*, vol. 16, no. 9, pp. 5689–5701, 2017.

[14] F. Sohrabi and W. Yu, "Hybrid digital and analog beamforming design for large-scale antenna arrays," *IEEE Journal of Selected Topics in Signal Processing*, vol. 10, no. 3, pp. 501–513, 2016.

[15] A. Alkhateeb, G. Leus, and R. W. Heath, "Compressed sensing based multi-user millimeter wave systems: how many measurements are needed?," in *2015 IEEE International Conference on Acoustics, Speech and Signal Processing (ICASSP), p*, pp. 2909–2913, South Brisbane, QLD, Australia, 2015.

[16] Y. Zeng, L. Yang, and R. Zhang, "Multi-user millimeter wave MIMO with full-dimensional lens antenna array," *IEEE Transactions on Wireless Communications*, vol. 17, no. 4, pp. 2800–2814, 2018.

[17] M. K. Samimi and T. S. Rappaport, "3-D statistical channel model for millimeter-wave outdoor mobile broadband communications," in *2015 IEEE International Conference on Communications (ICC)*, pp. 2430–2436, London, UK, 2015.

[18] C. Lin, G. Y. Li, and L. Wang, "Subarray-based coordinated beamforming training for mmWave and sub-THz communications," *IEEE Journal on Selected Areas in Communications*, vol. 35, no. 9, pp. 2115–2126, 2017.

[19] J. Hou, Y. Deng, and M. Shikh-Bahaei, "Joint beamforming, user association, and height control for cellular-enabled UAV communications," *IEEE Transactions on Communications*, vol. 69, no. 6, pp. 3598–3613, 2021.

[20] Y. Cho and J. Kim, "Line-of-sight MIMO channel in millimeter-wave beamforming system: modeling and prototype results," in *2015 IEEE 81st Vehicular Technology Conference (VTC Spring)*, Glasgow, UK, 2015.

[21] S. A. Busari, K. M. S. Huq, S. Mumtaz, L. Dai, and J. Rodriguez, "Millimeter-wave massive MIMO communication for future wireless systems: a survey," *IEEE Communications Surveys & Tutorials*, vol. 20, no. 2, pp. 836–869, 2018.

[22] Y. Han, S. Jin, J. Zhang, J. Zhang, and K. K. Wong, "DFT-based hybrid beamforming multiuser systems: rate analysis and beam selection," *IEEE Journal of Selected Topics in Signal Processing*, vol. 12, no. 3, pp. 514–528, 2018.

[23] F. Khalid, "Hybrid beamforming for millimeter wave massive multiuser MIMO systems using regularized channel diagonalization," *IEEE Wireless Communications Letters*, vol. 8, no. 3, pp. 705–708, 2019.

[24] H. Ren, L. Li, W. Xu, W. Chen, and Z. Han, "Machine learning-based hybrid precoding with robust error for UAV

mmWave massive MIMO," in *ICC 2019-2019 IEEE International Conference on Communications (ICC)*, Shanghai, China, 2019.

[25] Z. Shen, K. Xu, and X. Xia, "2D fingerprinting-based localization for mmWave cell-free massive MIMO systems," *IEEE Communications Letters*, vol. 25, no. 11, pp. 3556–3560, 2021.

[26] Z. Shen, K. Xu, X. Xia, W. Xie, and D. Zhang, "Spatial sparsity based secure transmission strategy for massive MIMO systems against simultaneous jamming and eavesdropping," *IEEE Transactions on Information Forensics and Security*, vol. 15, pp. 3760–3774, 2020.

[27] Z. Shen, K. Xu, and X. Xia, "Beam-domain anti-jamming transmission for downlink massive MIMO systems: a Stackelberg game perspective," *IEEE Transactions on Information Forensics and Security*, vol. 16, pp. 2727–2742, 2021.

[28] Y. Ding and A. Hu, "Grouping optimization based hybrid beamforming for multiuser MmWave massive MIMO systems," in *2019 IEEE 2nd International Conference on Computer and Communication Engineering Technology (CCET)*, pp. 203–207, Beijing, China, 2019.

[29] P. V. Amadori and C. Masouros, "Low RF-complexity millimeter-wave beamspace-MIMO systems by beam selection," *IEEE Transactions on Communications*, vol. 63, no. 6, pp. 2212–2223, 2015.

[30] A. Alkhateeb, G. Leus, and R. W. Heath, "Limited feedback hybrid precoding for multi-user millimeter wave systems," *IEEE Transactions on Wireless Communications*, vol. 14, no. 11, pp. 6481–6494, 2015.

[31] Y. Sun and C. Qi, "Weighted sum-rate maximization for analog beamforming and combining in millimeter wave massive MIMO communications," *IEEE Communications Letters*, vol. 21, no. 8, pp. 1883–1886, 2017.

[32] X. Huang, W. Xu, G. Xie, S. Jin, and X. You, "Learning oriented cross-entropy approach to user association in load-balanced HetNet," *IEEE Wireless Communications Letters*, vol. 7, no. 6, pp. 1014–1017, 2018.

[33] M. Kokshoorn, H. Chen, Y. Li, and B. Vucetic, "Beam-on-graph: simultaneous channel estimation for mmWave MIMO systems with multiple users," *IEEE Transactions on Communications*, vol. 66, no. 7, pp. 2931–2946, 2018.

[34] W. Zhang, W. Zhang, and J. Wu, "UAV beam alignment for highly mobile millimeter wave communications," *IEEE Transactions on Vehicular Technology*, vol. 69, no. 8, pp. 8577–8585, 2020.

[35] Z. Xiao, T. He, P. Xia, and X. G. Xia, "Hierarchical codebook design for beamforming training in millimeter-wave communication," *IEEE Transactions on Wireless Communications*, vol. 15, no. 5, pp. 3380–3392, 2016.

[36] K. Xu, F. C. Zheng, P. Cao, H. Xu, and X. Zhu, "Fast 3D beam training in mmWave multiuser MIMO systems with finite-bit phase shifters," in *ICC 2020-2020 IEEE International Conference on Communications (ICC)*, Dublin, Ireland, 2020.

[37] L. Chiu and S. Wu, "Hybrid radio frequency beamforming and baseband precoding for downlink MU-MIMO mmWave channels," in *2015 IEEE International Conference on Communications (ICC)*, pp. 1346–1351, London, UK, 2015.

[38] L. Liang, W. Xu, and X. Dong, "Low-complexity hybrid precoding in massive multiuser MIMO systems," *IEEE Wireless Communications Letters*, vol. 3, no. 6, pp. 653–656, 2014.

[39] A. Alkhateeb, Y. Nam, J. Zhang, and R. W. Heath, "Massive MIMO combining with switches," *IEEE Wireless Communications Letters*, vol. 5, no. 3, pp. 232–235, 2016.

[40] S. Buzzi and C. D'Andrea, "Doubly massive mmWave MIMO systems: using very large antenna arrays at both transmitter and receiver," in *2016 IEEE Global Communications Conference (GLOBECOM)*, Washington, DC, USA, 2016.

[41] T. S. Rappaport, G. R. MacCartney, M. K. Samimi, and S. Sun, "Wideband millimeter-wave propagation measurements and channel models for future wireless communication system design," *IEEE Transactions on Communications*, vol. 63, no. 9, pp. 3029–3056, 2015.

[42] J. Choi, "Beam selection in mm-wave multiuser MIMO systems using compressive sensing," *IEEE Transactions on Communications*, vol. 63, no. 8, pp. 2936–2947, 2015.

[43] F. Dong, W. Wang, Z. Huang, and P. Huang, "High-resolution angle-of-arrival and channel estimation for mmWave massive MIMO systems with lens antenna array," *IEEE Transactions on Vehicular Technology*, vol. 69, no. 11, pp. 12963–12973, 2020.

[44] I. Ahmed, K. Shahid, F. Debretsion, H. Khammari, and K. Alnajjar, "Energy efficiency of multiuser sparse massive MIMO system using orthogonalized hybrid beamforming," in *2021 IEEE 93rd Vehicular Technology Conference (VTC2021-Spring)*, Helsinki, Finland, 2021.

[45] D. Arora and M. Rawat, "Hybrid beamforming utilization perspective for future 5G millimeter wave communication," in *2017 IEEE International WIE Conference on Electrical and Computer Engineering (WIECON-ECE)*, pp. 149–152, Dehradun, India, 2017.